

Quasi-Conformal Hybrid Multi-modality Image Registration and its Application to Medical Image Fusion

Ka Chun Lam^(✉) and Lok Ming Lui

Department of Mathematics, The Chinese University of Hong Kong,
Room 220, Lady Shaw Building, Shatin N.T., Hong Kong, China
jefferykclam@gmail.com, lmlui@math.cuhk.edu.hk

Abstract. Fusion of images with same or different modalities has been conquering medical imaging field more rapidly due to the presence of highly accessible patients' information in recent years. For example, cross platform non-rigid registration of CT with MRI images has found a significant role in different clinical application. In some instances labelling of anatomical features by medical experts are also involved to further improve the accuracy and authenticity of the registration. Being motivated by these, we propose a new algorithm to compute diffeomorphic hybrid multi-modality registration with large deformations. Our iterative scheme consists of mainly two steps. First, we obtain the optimal Beltrami coefficient corresponding to the diffeomorphic mapping that exactly superimposes the feature points. The second step detects the intensity difference in the framework of mutual information. A non-rigid deformation which minimizes the intensity difference is then obtained. Experiments have been carried out on both synthetic and real data. Results demonstrate the stability and efficacy of the proposed algorithm to obtain diffeomorphic image registration.

1 Introduction

Image registration is one of the important steps in various fields which aims to align images [1–3]. Existing methods for image registration can be classified into three categories: landmark-based, intensity-based and hybrid methods. For landmark-based method, optimal deformation is obtained by aligning the sparse geometric feature points on both source and target domain. For example, the thin-plate spline registration method proposed by Bookstein et al. [4] aligns landmarks by using the biharmonic regularizer. Later, Joshi et al. [5] proposed to obtain the landmark matching diffeomorphism through the construction of vector field governed by the Navier-Stokes equation. A diffeomorphism with exact landmark alignment can be computed even with large deformation. One main advantages of landmark-based method is the straightforward incorporation of medical expert during the registration process [2]. This provides a reliable deformation approximation once the features alignment is accurate. In addition, landmark-based method is usually computationally efficient when

modelling large deformations. Intensity-based registration method aims to match the intensity information without the help of sparse geometric knowledge. By taking into account more image information during the registration process, delineation of feature landmarks is not required. To list a few, the Diffeomorphic Demons Registration method in [6], which is proposed based on Thirion's demons algorithm [7], obtains the registration result in the space of diffeomorphic transformations. Glocker proposed the DROP algorithm [8] to register images by making use of the Markov random field formulation. But without human supervision, inaccurate registration with underlying large deformation may be resulted. Hybrid approaches make use of both sparse geometric and intensity information to guide the registration. By aligning landmark and intensity, we integrate both merits of matching approaches: reliability of meaningful feature alignment provided by medical practitioners and accurate registration of local intensity information. As a consequence, this type of approach can usually provide better registration results. For instance, Christensen et al. [9] proposed to apply the unidirectional landmark thin-plate-spline (UL-TPS) registration technique with the minimization of intensity difference to register images with inverse consistency property. Chanwimaluang et al. [10] proposed a hybrid retina image registration by the combination of area-based and feature-based alignment techniques.

A large amount of work has also been published on medical image fusion recently [11] due to the increasing use of medical diagnostic devices and the improved accessibility of medical data. There are mainly two stages: (1) image registration and (2) fusion of image information from the registered images [11]. In the fusion part, various methods have been proposed. To name a few, Li et al. [12] combine images under the space of wavelet coefficients. The integrated images is obtained by taking the inverse wavelet transform of the fused wavelet coefficients. Naidu et al. [13] proposed to use principal component analysis (PCA) to obtain a weighted average for the registered images to be fused.

In this paper, we extend the landmark matching algorithm in [14] to obtain diffeomorphic hybrid image registration which can handle different modalities. The main idea of the algorithm is to find the optimizer of an energy functional involving the Beltrami coefficients term, which is effective in controlling the bijectivity and the conformality distortion of the mapping. Diffeomorphism associated to the optimized Beltrami coefficient will satisfy the landmark constraints and maximize the mutual information between the source and target images. In addition, our proposed algorithm can also control the conformality distortion of the transformation. The obtained transform thus preserves as much local geometric information as possible. Noted that an accurate diffeomorphic alignment is also a key issue as severe artefact in the fused image may be produced due to misalignment or loss of image information in folding regions. We therefore propose to restrict the class of registration transformation to Quasi-Conformal mapping for image fusion problem. To validate the scheme, we have tested it on different synthetic examples and real medical images. Results show that our proposed algorithm can successfully align images according to the prescribed landmark constraints and the similarity of image intensity. The use of our

registration result can improve the image fusion quality and place a significant amount of trust under the inclusion of experts' labelling.

2 Mathematical Background

Our algorithm obtains the optimal transformation in the class of Quasi-Conformal (QC) mapping. QC maps are generalization of conformal maps which are orientation preserving homeomorphisms between Riemann surfaces with bounded conformality distortion. Mathematically, let $z = x + \sqrt{-1}y$ with $x, y \in \mathbb{R}$, $f : \mathbb{C} \rightarrow \mathbb{C}$ is a QC map if it satisfies the following Beltrami equation:

$$\frac{\partial f}{\partial \bar{z}} = \mu(z) \frac{\partial f}{\partial z} \quad (1)$$

for some complex-valued function μ satisfying $\|\mu\|_\infty < 1$. The function μ is called the Beltrami coefficient, which measures the nonconformality of the mapping f . By the first order Taylor expansion $f(z) \approx f(p) + f_z(p)(z - p + \mu(p)(\bar{z} - \bar{p}))$, the Beltrami coefficient provides us all the information about the conformality of the mapping. In addition, the following theorem describes the relation between the set of Beltrami coefficients and the set of orientation preserving homeomorphisms (See [15] for details).

Theorem 1. *Suppose $\mu : \mathbb{D} \rightarrow \mathbb{D}$ is Lebesgue measurable satisfying $\|\mu\|_\infty < 1$, then there is a Quasi-Conformal homeomorphism ϕ from the unit disk to itself, which is in the Sobolev space $W^{1,2}(\Omega)$ and satisfies the Beltrami equation (1) in the distribution sense. Furthermore, by fixing 0 and 1, the associated Quasi-Conformal homeomorphism ϕ is uniquely determined.*

This theorem motivates us to transform the problem of finding the optimal deformation into the problem of finding the corresponding Beltrami coefficient. The following theorem helps us to understand the relationship between the regularity of the Beltrami coefficient $\mu(f)$ and the associated mapping f .

Theorem 2. *For any smooth μ with $\|\mu\|_\infty < 1$, the corresponding Quasi-Conformal homeomorphism f is a C^∞ diffeomorphism.*

To measure the similarity of two images with different modalities, we apply the mutual transform proposed by Kroon [16]. Let M and S be the moving and the static image. The mutual transform M_T of M to S is defined to be

$$M_T(x) = \arg \max_K H_{G_x^r}(M, S, K) \quad (2)$$

where x is the pixel position in the image; K is the intensity level; G_x^r is the Gaussian windows with center x and radius r and $H_{G_x^r}(M, S, K)$ is the number of pixel in G_x^r of intensity matrix $M(x)$, which is linked to intensity level K in the static image S . With mutual transform, we define the similarity measurement to be:

$$\text{Similar}(M, S) = \frac{1}{2} \int_{\Omega} (S_T - M)^2 + \frac{1}{2} \int_{\Omega} (S - M_T)^2 \quad (3)$$

where Ω is the domain of the image M .

3 Methodology

We now formulate the hybrid multi-modality registration problem as the following mathematical model. Let M and S to be the moving image and the static image respectively. Denote $\{p_i\}_{i=1,\dots,m} \in M$ and $\{q_i\}_{i=1,\dots,m} \in S$ to be the prescribed landmark correspondences. We also let $\mu(f) = \frac{\partial f}{\partial \bar{z}} / \frac{\partial f}{\partial z}$ and f_μ to be the solution f of the Beltrami equation (1) with Beltrami coefficient μ . The registration problem can be modelled as follows:

$$f = \arg \min_g \text{Similar}(M \circ g), \quad g : M \rightarrow S; \tag{4}$$

subject to:

- f is diffeomorphic;
- f satisfies the landmark constraints: $f(p_i) = q_i$ for $i = 1, \dots, m$;

It is well-known that restricting the transformation to be bijective is difficult. However, by the Quasi-Conformal theory, there is a one-one correspondence between the set of Beltrami coefficients and the set of Quasi-conformal homeomorphisms. Therefore, we avoid to find the optimal deformation f by optimizing the associated Beltrami coefficient instead. In other words, we have the following energy-based variational framework for solving the hybrid multi-modality registration problem:

$$(\bar{\mu}, f) = \arg \min_{\nu, g} \int_{\Omega} |\nabla \nu|^2 + \alpha \int_{\Omega} |\nu|^p + \frac{1}{2} \left[\int_{\Omega} (S_T - M \circ g)^2 + \int_{\Omega} (S - M_T \circ g)^2 \right]$$

subject to:

- $\|\bar{\mu}\|_{\infty} < 1$;
- $f(p_i) = q_i \forall i = 1, 2, \dots, m$;
- $\mu(f) = \bar{\mu}$.

To solve this minimization problem, we propose to use the penalty splitting method. We consider to minimize:

$$(\bar{\mu}, \bar{\nu}) = \arg \min_{\nu, \mu} \int_{\Omega} |\nabla \nu|^2 + \alpha \int_{\Omega} |\nu|^p + \sigma \int_{\Omega} |\nu - \mu|^2 + \frac{1}{2} \beta \left[\int_{\Omega} (S_T - M \circ g_\mu)^2 + \int_{\Omega} (S - M_T \circ g_\mu)^2 \right]$$

and subject to $\|\bar{\mu}\|_{\infty} < 1$ and $g_{\bar{\mu}}(p_i) = q_i \forall i = 1, 2, \dots, m$.

Different from the ordinary penalty method, we fix σ to be a large enough constant to improve the efficiency of the algorithm. We have also set $p = 2$ to ensure $\|\bar{\mu}\|_{\infty} < 1$ in practice. Experiments show that this simplification can give satisfactory result even with large deformation.

μ -Subproblem

We first discuss the minimization problem over μ fixing ν_n :

$$\mu_{n+1} = \arg \min_{\mu} \left\{ \frac{1}{2} \beta \left[\int_{\Omega} (S_T - M \circ g_{\mu})^2 + \int_{\Omega} (S - M_T \circ g_{\mu})^2 \right] + \sigma \int_{\Omega} |\nu_n - \mu|^2 \right\} \quad (5)$$

To solve the minimization problem, we applied the modified Demon's algorithm proposed by Kroon [16] to obtain the descent direction dg_{μ} which minimizes $\int_{\Omega} (S_T - M \circ g_{\mu})^2 + \int_{\Omega} (S - M_T \circ g_{\mu})^2$:

$$\begin{aligned} dg_{\mu} = & (M_T \circ g_{\mu} - S) \left(\frac{\nabla M_T}{|\nabla S|^2 + \phi^2 (M_T \circ g_{\mu} - S)^2} \right) \\ & + (M \circ g_{\mu} - S_T) \left(\frac{\nabla M}{|\nabla M|^2 + \phi^2 (M \circ g_{\mu} - S_T)^2} \right) \end{aligned}$$

The modified Demon's direction provide us the adjustment of the mapping dg_{μ} which minimizes the energy functional. Theoretically, we know that g_{μ} is perturbed by $g(t) = g_{\mu} + tdg_{\mu} + o(|t|)$, in which

$$\begin{aligned} dg_{\mu}(p) = & - \frac{g_{\mu}(g_{\mu}(p) - 1)}{\pi} \left(\int_{\Omega} \frac{d\mu_1(z)((g_{\mu})_z(z))^2}{g_{\mu}(z)(g_{\mu}(z) - 1)(g_{\mu}(z) - g_{\mu}(p))} dx dy \right. \\ & \left. + \int_{\Omega} \frac{\overline{d\mu_1(z)((g_{\mu})_z(z))^2}}{g_{\mu}(z)(1 - g_{\mu}(z))(1 - g_{\mu}(z)g_{\mu}(p))} dx dy \right) \end{aligned}$$

when μ is perturbed by $\mu = \mu + td\mu_1 + t\epsilon(t)$, where $\|\epsilon(t)\|_{\infty} \rightarrow 0$ as $t \rightarrow 0$. However, it is inefficient to obtain $d\mu_1$ from the above equality. Instead, we consider the first order approximation:

$$\frac{\partial(g_{\mu} + dg_{\mu})}{\partial \bar{z}} = (\mu + d\mu_1) \frac{\partial(g_{\mu} + dg_{\mu})}{\partial z} \quad (6)$$

By further substituting the Beltrami equation in (1), we have

$$d\mu_1 = \left(\frac{\partial dg_{\mu}}{\partial \bar{z}} - \mu \frac{\partial dg_{\mu}}{\partial z} \right) / \frac{\partial(g_{\mu} + dg_{\mu})}{\partial z} \quad (7)$$

For the second term, the descent direction is simply

$$d\mu_2 = -2(\mu - \nu_n) \quad (8)$$

Therefore, the overall descent direction for the μ -subproblem is given by

$$d\mu = \frac{1}{2} \beta d\mu_1 + \sigma d\mu_2 \quad (9)$$

With the updated Beltrami coefficient $\tilde{\mu}_{n+1} = \mu_n + td\mu$ for some step size t , we then solve the Beltrami equation for $f_{n+\frac{1}{2}}$ in least square sense with given Beltrami coefficients $\tilde{\mu}_{n+1}$ and landmark constraints to ensure that feature points can be superimposed exactly after the registration. The detail for solving the Beltrami equation will be discussed in Sect. 4. Once $f_{n+\frac{1}{2}}$ is calculated, we obtain the local minimum $\mu_{n+1} = \mu(f_{n+\frac{1}{2}})$ of the sub-problem.

ν -Subproblem

After updating μ , we optimize the energy function over ν fixing μ_{n+1} :

$$\tilde{\nu}_{n+1} = \arg \min_{\nu} \int_{\Omega} |\nabla \nu|^2 + \alpha \int_{\Omega} |\nu|^2 + \sigma \int_{\Omega} |\nu - \mu_{n+1}|^2 \tag{10}$$

A straightforward calculation shows that the Euler-Lagrange equation of the above energy function is

$$(-\Delta + 2\alpha I + 2\sigma I)\tilde{\nu}_{n+1} = \mu_{n+1} \tag{11}$$

Similar to the case of μ -subproblem, the Beltrami coefficient $\tilde{\nu}_{n+1}$ obtain from solving (11) is used to solve the Beltrami equation together with landmark constraints. This updates the $\nu_{n+1} = \mu(f_{n+1})$ in which the associated deformation f_{n+1} will match the prescribed feature points. We then keep the iteration going to obtain a sequence of pairs $\{(\mu_n, \nu_n)\}_n$. Iteration stops when $\|\nu_{n+1} - \nu_n\| \leq \epsilon$ for some threshold ϵ .

4 Implementation

We now describe the numerical implementation of our proposed algorithm.

Solving the Beltrami Equation

Given the Beltrami coefficient μ and the landmark constraints, we need to solve (1) for f_{μ} which closely resembles to the given μ and satisfies $f(p_i) = q_i$. We follow the idea in [17,18] to transform the Beltrami equation into an elliptic partial differential equation and discretize it by using finite element method:

$$\nabla \cdot \left(A \begin{pmatrix} u_x \\ u_y \end{pmatrix} \right) = 0; \quad \nabla \cdot \left(A \begin{pmatrix} v_x \\ v_y \end{pmatrix} \right) = 0, \quad \text{where } A = \begin{pmatrix} \frac{(\rho-1)^2 + \tau^2}{1-\rho^2-\tau^2} & -\frac{2\tau}{1-\rho^2-\tau^2} \\ -\frac{2\tau}{1-\rho^2-\tau^2} & \frac{1+2\rho+\rho^2+\tau^2}{1-\rho^2-\tau^2} \end{pmatrix} \tag{12}$$

A linear system with symmetric positive definite matrix can be formulated after discretization. We can then impose the landmark constraints and solve for a least square solution.

Choice of Parameters

For the step size appears in the μ -subproblem, we adopted an approximation of the Barzilai and Borwein approach [19] to set the step size t :

$$t = \frac{(dg_{\mu_{n+1}} - dg_{\mu_n})^T (\mu_{n+1} - \mu_n)}{(dg_{\mu_{n+1}} - dg_{\mu_n})^T (dg_{\mu_{n+1}} - dg_{\mu_n})} \tag{13}$$

The parameter α controls the conformality distortion of the deformation and we set $\alpha = 0.1$. The parameter β is responsible for the matching for the intensity similarity. We set $\beta = 1$. The penalty parameter σ is set to 10 which is large enough for all experiments we reported in the next session. The threshold ϵ is set to 0.05 for optimal solution.

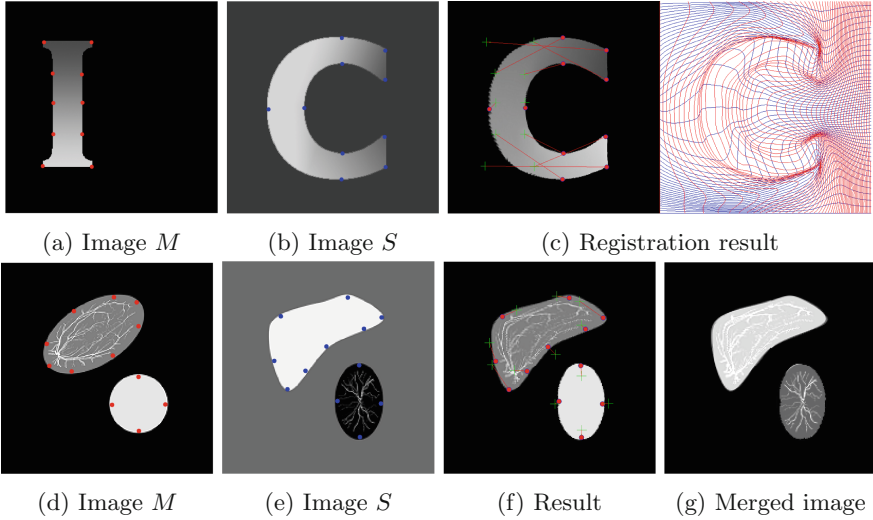


Fig. 1. Image registration of Example 1((a)–(c)) and Example 2((d)–(g)) respectively (Color figure online).

Image Fusion

Once we have the registered image $f(M)$, we can integrate the two images by using different well-established method. In this work, we adopted the Discrete wavelet transform (DWT) fusion method [12] to integrate the registered images. The main idea of this method is to merge the wavelet decomposition of the two images in the transformed domain. Since a larger absolute value of the coefficients correspond to some salient features in the images, important features on images can be integrated by the fusion of wavelet coefficients effectively.

5 Experimental Result

To validate the efficacy of our algorithm, we have tested it on both synthetic data together with the real medical data.

Example 1: In the first example, we validate our proposed algorithm by registering an image with English character “I” to an image with English character “C” with different modalities. Figure 1(a) and (b) show the moving image with character “I” and the static image with character “C” respectively. The red and blue dots on the images illustrate the prescribed landmark criteria $f(p_i) \rightarrow q_i, i = 1, \dots, m$ in the registration. The green cross in (c) shows the original landmark position in (a), which indicates that a large displacement is present in this registration problem. By using our proposed algorithm, a large diffeomorphic transformation f superimposing the feature points and maximizing the intensity similarity is obtained. The registered result is shown in Fig. 1(c).

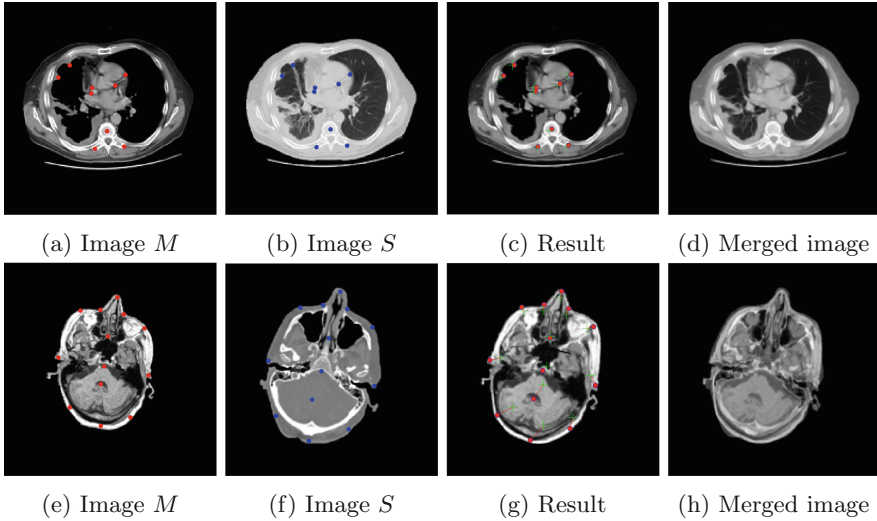


Fig. 2. Medical image registration and fusion of Example 3((a)–(d)) and Example 4((e)–(h)) respectively (Color figure online).

Example 2: Figure 1(d) and (e) shows the moving image M and S respectively. Synthetic blood vessels are planted in both images. The registered result is shown in (f), which is constructed by deforming the moving image M to superimpose S with maximum intensity similarity. The green cross indicates the original landmarks position in (d). The registered image and the static image S are then combined to have the fusion image (g). Note that the blood vessels from both images are integrated. In other words, local information from both images are merged together.

Example 3: We have also tested our algorithm with real medical images. Figure 2(a)–(d) shows an example of image fusion of a lung MRI image and a lung CT image. Figure 2(a) and (b) show the moving and static image M and S respectively. By the proposed algorithm, we obtained the registration result, which is shown in (c). By using the fusion technique discussed in Sect. 4, we have the integrated image (d). Note that the detail of blood vessels in image S and the detail of the heart in image M are both included in the integrated image. This shows that our proposed algorithm can effectively align the images with different modalities.

Example 4: In this example, we validate our proposed algorithm on the image registration between brain MRI and CT images. Figure 2(e) and (f) show the MRI and CT brain images respectively. The red and blue dots represent the artificial landmark constraints for testing purpose. We have set the parameter $\alpha = 1$ due to the highly dissimilarity of the intensity distribution. This prevents the perturbation of local deformation created by mismatching of intensity. In other words, conformality distortion contributes a larger portion in the energy

Table 1. Summary of the registration results using different registration methods

			Landmark [14]		MI [16]		Proposed	
	LM_{\max}	LM_{mean}	e_{\max} $\ \mu\ _{\infty}$	e_{mean} MI	e_{\max} $\ \mu\ _{\infty}$	e_{mean} MI	e_{\max} $\ \mu\ _{\infty}$	e_{mean} MI
Example 1	0.3309	0.1293	0	0	0.3078	0.1140	0	0
			0.9950	0.5324	0.9993	0.1781	0.9775	1.0736
Example 2	0.0196	0.0057	0	0	0.0176	0.0062	0	0
			0.7295	0.8088	0.9061	0.8311	0.8807	0.9712
Example 3	0.0023	0.0013	0	0	$2.42e^{-3}$	$1.73e^{-3}$	0	0
			0.4126	1.3806	0.4126	1.4787	0.2220	1.4758
Example 4	0.0087	0.0027	0	0	0.0094	0.0037	0	0
			0.4650	1.1929	0.5243	0.8670	0.4126	1.2025

functional under this setting and so the registration is less sensitive to the intensity difference. Figure 2(g) shows the registration result. It demonstrates that our proposed algorithm can align images with different modalities well, which is also illustrated by the image fusion result as shown in (h).

To validate our proposed algorithm, we compare the results obtained with landmark-based image registration method proposed in [14] and the multi-modality image registration in [16]. Quantitative measures are reported in Table 1. We first normalize the image domain into the $[0, 1] \times [0, 1]$ domain. LM_{\max} and LM_{mean} represent the maximum and mean landmark displacement in the example respectively. e_{\max} and e_{mean} measure the maximum and the mean error of the landmark alignment. Note that method in [16] is intensity-based and so landmark mismatching errors always exist. $\|\mu\|_{\infty}$ measures the maximum value of the conformality distortion. $\|\mu\|_{\infty} < 1$ indicates that the mapping is diffeomorphic. MI measures the mutual information between the target image and the deformed image. A larger MI value implies a more accurate image superimposition is achieved. The table shows that our proposed algorithm can accurately align landmarks exactly and maximize the mutual information during the registration.

6 Conclusion

In this work, an iterative scheme is proposed to register images with different modalities under prescribed landmark constraints. The main idea of our method is to find an optimized Beltrami coefficients for which the associated diffeomorphism satisfies the landmark constraints and superimposes the intensities in the sense of similarity of the images. We have applied our algorithm to register medical images with different modalities for image fusion. Experimental results show that our proposed algorithm can align images and match landmarks well, which is important for obtaining accurate image fusion.

Acknowledgements. This project is supported by HKRGC GRF (Project ID: 2130363 Reference: 402413)

References

1. Heckbert, P.S.: Survey of texture mapping. *IEEE Comput. Graphics Appl.* **6**, 56–67 (1986)
2. Sotiras, A., Davatzikos, C., Paragios, N.: Deformable medical image registration: a survey. *IEEE Trans. Med. Imaging* **32**, 1153–1190 (2013)
3. Zitova, B., Flusser, J.: Image registration methods: a survey. *Image Vis. Comput.* **21**, 977–1000 (2003)
4. Bookstein, F.L.: Principal warps: thin-plate splines and the decomposition of deformations. *IEEE Trans. Pattern Anal. Mach. Intell.* **11**, 567–585 (1989)
5. Joshi, S.C., Miller, M.I.: Landmark matching via large deformation diffeomorphisms. *IEEE Trans. Image Process.* **9**, 1357–1370 (2000)
6. Vercauteren, T., Pennec, X., Perchant, A., Ayache, N.: Diffeomorphic demons: efficient non-parametric image registration. *NeuroImage* **45**, S61–S72 (2009)
7. Thirion, J.P.: Image matching as a diffusion process: an analogy with Maxwell’s demons. *Med. Image Anal.* **2**, 243–260 (1998)
8. Glocker, B., Sotiras, A., Komodakis, N., Paragios, N.: Deformable medical image registration: setting the state of the art with discrete methods. *Annu. Rev. Biomed. Eng.* **13**, 219–244 (2011)
9. Christensen, G.E., Johnson, H.J.: Consistent image registration. *IEEE Trans. Med. Imaging* **20**, 568–582 (2001)
10. Chanwimaluang, T., Fan, G., Fransen, S.R.: Hybrid retinal image registration. *IEEE Trans. Inf. Technol. Biomed.* **10**, 129–142 (2006)
11. James, A., Dasarathy, B.: Medical image fusion: a survey of the state of the art. *Inf. Fusion* **19**, 4–19 (2014)
12. Li, H., Manjunath, B., Mitra, S.: Multisensor image fusion using the wavelet transform. *Graph. Models Image Process.* **57**, 235–245 (1995)
13. Naidu, V., Raol, J.: Pixel-level image fusion using wavelets and principal component analysis. *Def. Sci. J.* **58**, 338–352 (2008)
14. Lam, K.C., Lui, L.M.: Landmark and intensity based registration with large deformations via quasi-conformal maps. *SIAM J. Imaging Sci.* **7**, 2364–2392 (2014)
15. Gardiner, F.P., Lakic, N.: *Quasiconformal Teichmüller Theory. Mathematical Surveys and Monographs.* American Mathematical Society, Providence (2000)
16. Kroon, D.: Multimodality non-rigid demon algorithm image registration. *Robust Non-rigid Point Matching* **14**, 120–126 (2008)
17. Astala, K., Iwaniec, T., Martin, G.: *Elliptic Partial Differential Equations and Quasiconformal Mappings in the Plane.* Oxford Graduate Texts in Mathematics. Princeton University Press, Princeton (2008)
18. Lui, L.M., Lam, K.C., Wong, T.W., Gu, X.F.: Texture map and video compression using Beltrami representation. *SIAM J. Imaging Sci.* **6**, 1880–1902 (2013)
19. Barzilai, J., Borwein, J.: Two-point step size gradient methods. *IMA J. Numer. Anal.* **8**, 141–148 (1988)